

A novel method for residual strength prediction for sheets with multiple site damage: Methodology and experimental validation



Wu Xu^{a,c}, Hai Wang^{a,*}, Xueren Wu^{b,a}, Xiaojing Zhang^a, Guojuan Bai^a, Xianglong Huang^a

^a School of Aeronautics and Astronautics, Shanghai Jiao Tong University, Shanghai 200240, China

^b AVIC Beijing Institute of Aeronautical Materials, Beijing 100095, China

^c Aerospace Engineering Department, University of Michigan, Ann Arbor, MI 48109, USA

ARTICLE INFO

Article history:

Received 4 April 2013

Received in revised form 3 October 2013

Available online 19 October 2013

Keywords:

Multiple site damage

Residual strength

Stable crack growth

Crack tip opening angle criterion

Strip yield model

Plastic zone size

Weight function method

ABSTRACT

A unified method for solving the strip yield model for collinear cracks in finite and infinite sheet is proposed. The method is based on the weight function of a single crack. Two collinear cracks in finite and infinite sheets are used to apply and verify this method. The plastic zone size, crack opening displacement and stress distribution along the ligament between cracks obtained by using the present method are extensively compared with existing available results and finite element solutions, and very good agreements are observed. Combined with the Crack Tip Opening Angle (CTOA) criterion, the unified method is used to predict the crack growth behavior and residual strength for 2024-T3 aluminum alloy sheet with Multiple Site Damage (MSD). Thirty-two sheets with four types of MSD are designed and tested to verify this method. It is shown that the present method is able to predict various crack growth behaviors observed in experiment. The predicted residual strengths are within 9% of the corresponding test results. Compared to the elastic–plastic finite element method, the present method is much more efficient.

© 2013 Elsevier Ltd. All rights reserved.

1. Introduction

Aircraft structures are designed to retain adequate structural integrity in the presence of major damage. The Aloha Airlines accident in 1988 resulted in much attention being paid to the Multiple Sites Damage (MSD) phenomenon of riveted lap joints in aircraft fuselages (Swift, 1994). MSD was characterized by the simultaneous presence of fatigue cracks in the same structural element, for example, fatigue cracking at multiple rivet locations in lap joints (FAA, 2010). Subsequently, procedures for maintaining the structural integrity of aging aircraft were established. However, there were still several civil and military aircraft failures reported due to the presence of Widespread Fatigue Damage (WFD) (FAA, 2010). In order to maintain the aircraft safety, in 2010, the Federal Aviation Administration (FAA) in US issued its newest rules to prevent catastrophic failure due to WFD throughout the operational life of certain existing transport category airplanes and all those to be certificated in the future (FAA, 2010). These incidents and the FAA requirements call for suitable methods to analyze the behaviors of multiple fatigue cracks in susceptible structural locations.

During the past two decades, various methodologies and fracture criteria had been developed to predict the residual strength

of MSD structures (Cherry et al., 1997; Jeong and Brewer, 1995; Labeas et al., 2005; Ma et al., 1996; Moukawsher et al., 1996; Wang et al., 1997; Smith et al., 2001). For thin aluminum alloy sheet, large plastic zone was observed in the residual strength analysis. Consequently, the well-established linear elastic fracture mechanics criterions were shown to be inaccurate or unable to predict the residual strength and stable crack growth for structures with MSD. The elastic–plastic fracture parameter, Crack Tip Opening Angle/Displacement (CTOA/D), was widely used to predict the residual strengths for stiffened and unstiffened panels with or without MSD (Dawicke and Newman, 1998; Hsu et al., 2003; Mahmoud and Lease, 2004; Newman et al., 2003a,b; Seshadri et al., 2003). In the practical application, the CTOA criterion was usually combined with elastic–plastic finite element method or the strip yield model. Many researchers had used the CTOA criterion and elastic–plastic finite element method to predict the stable crack growth behaviors and residual strengths for various cracked configuration. Most of the predicted results were reported to be within 10% of the experimental data. However, when finite element method was involved, large computational and modeling demands as well as experiences were required. Since Dugdale (1960) strip yield model is relative simple to calculate the plastic zone size and crack opening displacement, it has been frequently combined with the CTOA criterion to predict the stable crack growth and residual strength (Deng and Hutchinson, 1996; Kuang and Chen, 2000; Nilsson and Hutchinson, 1994; Nilsson, 1999). And various methods were

* Corresponding author. Tel.: +86 2134206629.

E-mail address: wanghai601@sina.com (H. Wang).

developed to solve the strip yield model for collinear cracks, for example, the complex stress function method (Collins and Cartwright, 2001), the Fredholm integral equation method (Nishimura, 2002). However, most existing analytical methods encounter difficulties especially in solution efficiency and in the ability of analyzing the effect of finite width on MSD, which cannot be ignored in the practical engineering analysis. Recently the weight function method (Wu and Carlsson, 1991) has been successfully used by the present writers to tackle the MSD problems (Wu and Xu, 2011; Xu et al., 2011; Xu and Wu, 2012).

In this paper, a simple and highly efficient analytical method based on the weight function of a single crack is proposed to analyze the strip yield models for collinear cracks, including the finite width effect. The strip yield models for two collinear cracks in infinite and finite sheets are taken as examples to demonstrate and verify the present method. The stress distributions along the ligament between cracks, the plastic zone sizes and crack opening displacements are determined. These results are extensively compared with those from previous studies and finite element results, and perfect agreements are observed. It is also observed that the present method is much simpler and more efficient than the other methods to analyze the strip yield model for collinear cracks. After the validation of the present method, it is combined with the CTOA criterion to predict the stable crack growth and residual strength for sheet with MSD subjected to tension loading. Thirty-two sheets made of 2024-T3 aluminum alloy with various MSD-patterns are designed and tested to verify the accuracy and efficiency of present method. It is shown that the present method is able to predict the stable crack growth behaviors well, and the predicted residual strengths are within 9% of the corresponding experimental results. Compared with elastic–plastic finite element method, the present method is much more efficient.

2. Residual strength prediction model

2.1. CTOA criterion based on strip yield model

The CTOA criterion combination with the strip yield model had been used by several researchers to predict the stable crack growth behavior (Deng and Hutchinson, 1996; Newman, 1986; Nilsson and Hutchinson, 1994; Nilsson, 1999). In the method, the crack growth was controlled by two parameters. One was the critical crack opening displacement δ_0 which was used to control the crack initiation; and the other was applied to characterize the stable crack growth behavior by a critical constant CTOA α_c .

A single crack configuration shown in Fig. 1 is taken as an example to describe the crack growth analysis criterion and process. The crack will be initiated when the crack tip opening displacement reaches the critical value δ_0 , see Fig. 1(a). Subsequently, it will grow forward. Fig. 1(b) shows the crack

opening profile when the crack has propagated a distance Δa . Plastic wake is left behind as the crack advances. The elastic deformation in the wake is much less than the plastic stretch. As a result, the height of the plastic wake can be approximated to be equal to the prior crack stretch. The further crack growth was controlled by the critical CTOA α_c . The crack opening angle was defined by the crack opening displacement at a small distance $d = 1$ mm behind the crack tip. When the crack tip opening angle reaches the critical value α_c , the crack will propagate a distance $d = 1$ mm. Consequently, the crack growth equation for the whole process is

$$\begin{cases} \delta(a_0, a_0) = \delta_0; & \text{crack initiation} \\ \delta(a, a-d) = 2d \tan(\alpha_c/2) + \delta_c(a-d, a-d); & \text{crack propagation} \end{cases} \quad (1)$$

where, $\delta(a, a-d)$ is the crack opening displacement at a distance d behind the crack tip, the first variable in the bracket is the current crack length, and the second is the x location. $\delta_c(a-d, a-d)$ is the plastic wake height, which is equal to the crack tip opening displacement. α_c is the critical crack opening angle.

Newman (1986) defined the right term in the second equation as crack tip opening displacement resistance curve V_R . Usually, the plastic wake increases with the crack growth, which results in the crack growth resistance. It was found (Newman, 1986) that the V_R curve was independent of the initial crack length, specimen width and geometrical type, but was a function of material and specimen thickness.

The criterion for a single crack was also adopted to predict the each crack growth for plates with MSD (Deng and Hutchinson, 1996; Galatolo and Nilsson, 2001; Nilsson and Hutchinson, 1994), see Fig. 2(a). The crack initiation criterion for sheets with MSD was

$$\delta(a_{0i}, a_{0i}) = \delta_0 \quad (2)$$

where a_{0i} is the i th crack length. And, the equations for propagation were

$$\begin{cases} \delta(a_i, a_i-d) = 2d \tan(\alpha_c/2) + \delta_c(a_i-d, a_i-d); & +x \text{ direction} \\ \delta(a_i, a_i+d) = 2d \tan(\alpha_c/2) + \delta_c(a_i+d, a_i+d); & -x \text{ direction} \end{cases} \quad (3)$$

Besides the crack initiation and propagation equation, a criterion for crack linkup (Fig. 2(b)) is needed to predict the crack growth behavior for sheets with MSD. Theoretically, the link-up criterion is the current ligament $l_i = 0$ mm. It is observed from experiment that the ligament will break immediately when the current ligament length l_i is small. Here, the equation for crack coalescence given in Galatolo and Nilsson (2001) is applied,

$$l_i \leq 2 \text{ mm}; \quad \text{ith ligament fracture} \quad (4)$$

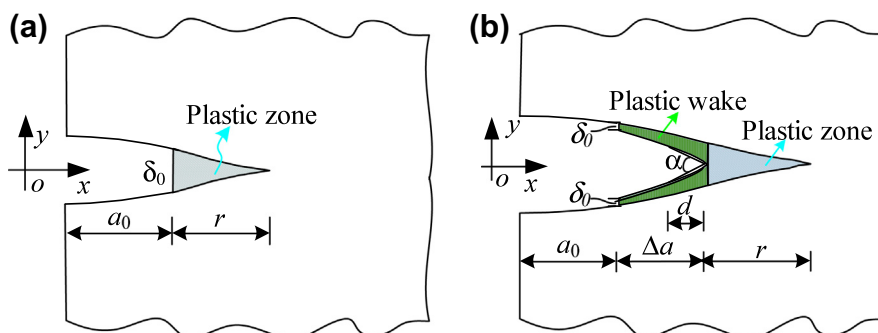


Fig. 1. Crack opening profile of modified Dugdale strip yield model at (a) initiation and (b) at propagation with definition of crack growth parameters α and δ_0 .

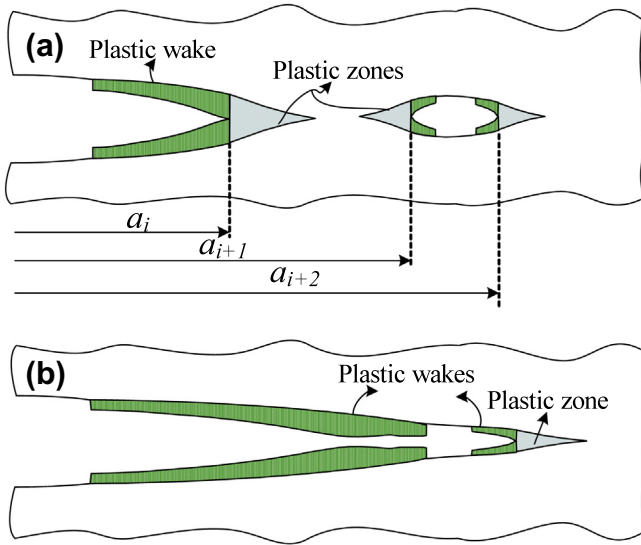


Fig. 2. Crack tip opening profile for multiple cracks; (a) before link-up (b) after ligament link-up.

After the coalescence of the cracks, a new crack is formed. If the crack tip has not been propagated, the crack initiation Eq. (2) will be used. Otherwise, the crack propagation criterion, Eq. (3) is applied.

2.2. Crack growth analysis procedure

The material properties and crack geometries are needed for the crack growth analysis. The basic material properties should be obtained from experiment. In the original strip yield model (Dugdale, 1960), the material was assumed to be perfect elastic plastic. In order to consider the plastic hardening in the strain–stress curve, an equation based on J -integral equivalent was proposed by Deng and Hutchinson (1996). However, in practical engineering application, the flow strength σ_Y is always used, which equals to $(\sigma_s + \sigma_u)/2$, σ_s and σ_u represent the yield and ultimate strength, respectively. For 2024-T3 aluminum, the results obtained from these two methods are nearly identical.

Essentially, crack growth analysis is the determination of the applied load to satisfy the crack initiation and growth equation. Since the plastic zone size and crack opening displacement are nonlinear functions of the applied load, the determination of the applied load is an iterative process. A flow chart for crack growth analysis is shown in Fig. 3. In order to describe it clearly, a single crack configuration is discussed first. For a given crack configuration a_0 subjected to applied load σ , the corresponding strip yield plastic zone size and crack opening displacement can be obtained by numerical or analytical method. The applied load σ is updated until the following equation is satisfied.

$$|\delta - \delta_c|/\delta_c \leq \varepsilon \quad (5)$$

where δ_c is δ_0 for crack initiation and V_R for crack growth, ε is a convergence norm, in the present study $\varepsilon = 10^{-4}$. Record this applied load and update the crack length ($a_0 = a_0 + d$) and critical crack opening displacement following Eq. (1). This process is repeated until the crack has been grown sufficiently long.

For sheets with multiple site cracks, the crack growth process follows nearly the same way as that for a single crack. The main differences are (1) $|\text{Max}[(\delta - \delta_c)/\delta_c]| < \varepsilon$ is used to determine which crack tip is to initiate or propagate; (2) Eq. (2) is used to update the critical opening displacement; and (3) Eq. (4) should be added in the flow chart to determine the linkup of the ligaments.

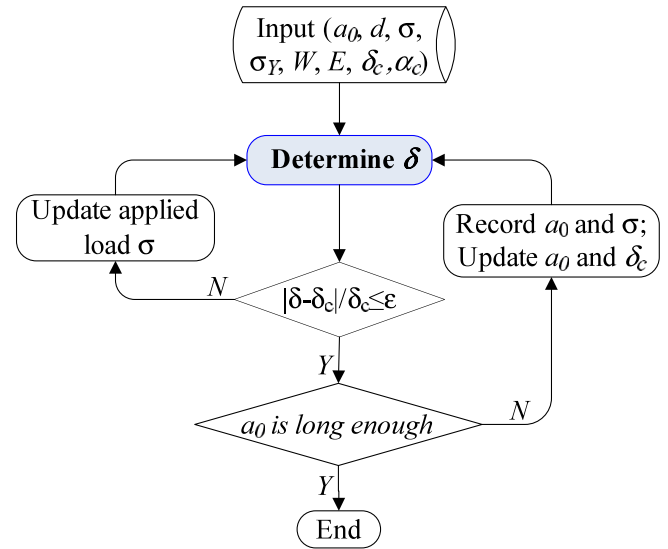


Fig. 3. Flow chart for crack growth analysis of a single crack.

3. A unified method for strip yield model solution to collinear cracks

It is observed from the flow chart in Fig. 3 that once the critical values δ_0 and α_c are available, the main task for crack growth analysis is to solve the strip yield model to obtain the crack opening displacement for cracked plates. As a result, the efficiency and accuracy of the crack growth analysis are much dependent on the method for solving the strip yield model.

Essentially, the Dugdale strip yield model is the superposition of two linear elastic solutions resulting from the remote applied load and compression yield stress acting over the strip yield zones. There were some methods proposed to solve the multiple collinear crack problems in infinite sheet. However, multiple collinear cracks problem in finite sheet is much more complicated than that in infinite sheet, and a few papers were focused on this topic (Chen and Wang, 2012). In the following, a unified method based on the weight function of a single crack is proposed to solve the strip yield model for collinear cracks in infinite and finite sheets.

3.1. The concept of the method

For simplicity but without loss of generality, the strip yield model for two collinear cracks in a finite sheet shown in Fig. 4(a) is taken as an example to illustrate the idea of the present method. The crack length is denoted by $2a$, and the ligament between these two cracks is $2b$. The plastic zone sizes and crack tip opening displacements for the inner and outer crack tips are denoted by r_A , r_B and δ_A , δ_B respectively. x and y are the Cartesian coordinates. Following the concept of Dugdale model, the plastic zone sizes are determined based on zero stress intensity factors at the fictitious crack tips and the equations are given by

$$f_i - f_{i,seg} = 0 \quad (6)$$

where f_i ($i = A, B$) are the non-dimensional stress intensity factors for the fictitious crack tips shown in Fig. 4(a) subjected to remote uniform tension stress σ ; $f_{i,seg}$ are the corresponding non-dimensional stress intensity factors for the fictitious cracks subjected to segments uniform compression yield stress $-\sigma_s$ over the plastic zones. Several methods had been proposed to obtain the stress intensity factors for cracks in infinite sheets. However, most of the methods

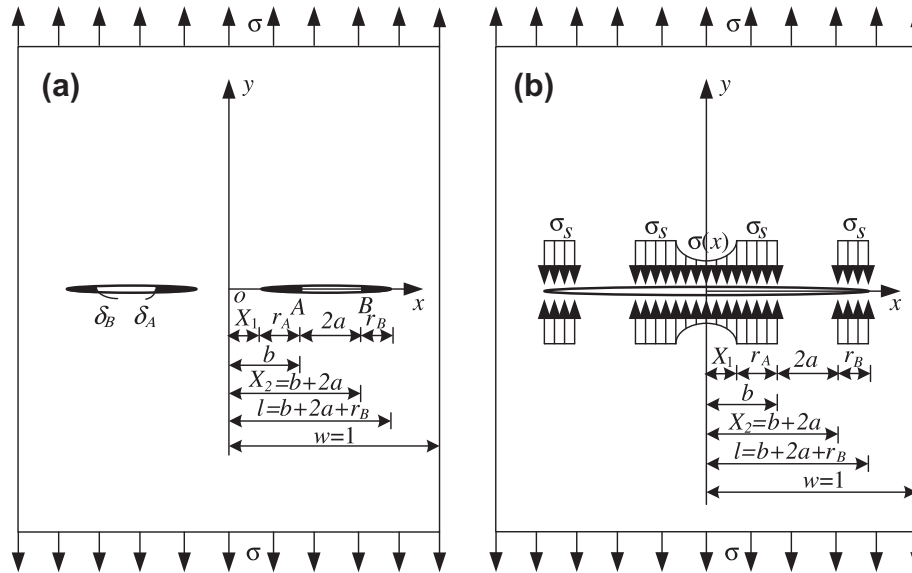


Fig. 4. An analytical model for solving the strip yield model for two equal-length collinear cracks in a finite sheet. (a) a strip yield model for two collinear cracks in a finite sheet; (b) an equivalent single center crack for modeling problem (a).

are very complicated and inefficient to obtain the stress intensity factors for collinear cracks in *finite* sheet under complex loading.

One of the key points of the present method is by treating all the cracks, plastic zones and ligaments between cracks as a single crack. For example, the strip yield model for two symmetric collinear cracks shown in Fig. 4(a) is modeled to be a single crack as shown in Fig. 4(b). The center crack of length $2l$ ($l = b + 2a + r_B$) is subjected to (i) remote uniform stress σ ; (ii) segments uniform compression yield stress $-\sigma_s$ over the plastic zones r_A and r_B ; and (iii) continuous compression stress $-\sigma(x)$ distributed along the remaining elastic ligament $x \in \pm[0, X_1]$, $X_1 = b - r_A$, respectively. The requirements for the equivalent single crack are:

- (1) No stress singularities at the crack tip, and
- (2) Zero crack opening displacements along the elastic ligament between the fictitious crack tips, $x \in \pm[0, X_1]$.

In order to solve the equivalent single crack problem, the unknown continuous stress $\sigma(x)$, $x \in \pm[0, X_1]$ is further modeled by a set of discrete value σ_i ($i = 1, 2, 3, \dots, N$) at the i th segment $[x_i, x_{i+1}]$ shown in Fig. 5. N is the total number of segment. The non-dimensional stress intensity factor $f(l, x_1, x_2)$ and crack opening displacement $u(l, x_1, x_2, x)$ for a *center crack in a finite sheet* subjected to segment uniform stress on the crack surface can be accurately and efficiently determined by using the weight function method (Fett and Munz, 1997; Wu and Carlsson, 1991). If the sheet is infinite, closed form results were collected in Tada et al. (2000). The expressions for stress intensity factor and crack opening displacement are given in Appendix A.

Using the superposition principle, the stress intensity factor F and crack opening displacement $U(l, x)$ for the equivalent single crack shown in Fig. 4(b) are

$$F = \sigma \cdot f(l, 0, l) - \sum_{i=1}^N \sigma_i \cdot f(l, x_i, x_{i+1}) - \sigma_s \cdot [f(l, X_1, b) + f(l, X_2, l)]; \quad x_i \in [0, X_1] \quad (7)$$

$$U(l, x) = \sigma \cdot u(l, 0, l, x) - \sum_{i=1}^N \sigma_i \cdot u(l, x_i, x_{i+1}, x) - \sigma_s \cdot [u(l, X_1, b, x) + u(l, X_2, l, x)]; \quad x_i \in [0, X_1] \quad (8)$$

And, the number of unknown variables becomes $(N + 2)$, which are σ_i ($i = 1, 2, 3, \dots, N$), r_A and r_B . In order to determine the unknown variables, the number of equations should be at least $(N + 2)$. Recalling the requirements for the equivalent crack, the following equations are established

$$\begin{cases} F = 0; \\ U(l, x) = 0; \quad x = (x_i + x_{i+1})/2, X_1; \quad i = 1, 2, 3, \dots, N \end{cases} \quad (9)$$

It is found that two approximations are introduced in Eq. (9): (i) the continuous stress distribution $\sigma(x)$ is modeled by a set of discrete uniform stress σ_i ; and (ii) zero crack opening displacement along the remaining elastic ligament between the fictitious crack tips are replaced by zero crack opening displacements at a set of discrete points along the elastic ligament. For most cases, the deviation caused by these two approximations can be reduced by the increase of segment number and proper arrangement. The segment

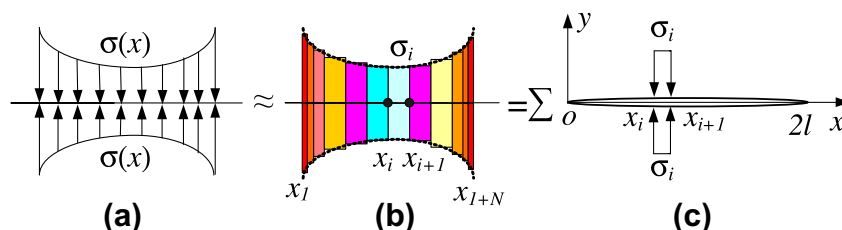


Fig. 5. A method used to model the effect of a continuous stress distribution.

length is gradually reduced to model the high stress gradient region shown in Fig. 5(b). In the present study, geometric sequence $\Delta x_i/x_{i-1} = q$ ($\Delta x_i = x_i - x_{i-1}$) is used to arrange the segments.

Having established the equations, Newton-iteration method is used to solve the plastic zone sizes and stress distribution $\sigma(x)$ along the elastic ligament. Subsequently, the corresponding crack opening displacement for the strip yield model can be obtained by using Eq. (8).

As the increase of the applied stress, the plastic zones become large and the elastic ligament will gradually reduce to zero. For the critical condition of plastic zones coalescence, the unknown variables are the plastic zone sizes r_B ($r_A = b$) and the critical applied stress σ_c . The requirements for this critical condition are: (1) no stress singularities at the crack tips and (2) the minimum crack opening displacement along the ligament $[0, b]$ is zero. In the present two equal-length collinear cracks, the second condition is equivalent to zero crack opening displacement at $x = 0$. Equations are established according to these conditions as follows

$$\begin{cases} F = 0 \\ U_{cr}(l, 0) = 0 \end{cases} \quad (10)$$

where,

$$F = \sigma \cdot f(l, 0, l) - \sigma_s \cdot [f(l, 0, b) + f(l, X_2, l)] \quad (11)$$

$$U_{cr}(l, x) = \sigma \cdot u(l, 0, l, x) - \sigma_s \cdot [u(l, 0, b, x) + u(l, X_2, l, x)] \quad (12)$$

The plastic zone sizes and critical applied stress can be obtained by solving the above equations. Having determined these values, the crack opening displacement for this case can be obtained according to Eq. (12). When the applied load σ is larger than the critical applied stress σ_c , the requirement is zero stress intensity factor for the equivalent crack. That is, Eq. (11) equals to zero. The only unknown variable is r_B , which is easy to solve.

For asymmetrical collinear cracks, if they are modeled as a single center crack as well, the corresponding equivalent center crack is usually eccentric. It is difficult to obtain the stress intensity factor and crack opening displacement solution to an eccentric crack subjected to complex loading, since accurate and efficient stress intensity factor and crack opening displacement solution to an eccentric crack subjected to segment uniform stress are unavailable. In order to solve this problem, the strip yield model for two general collinear cracks is modeled as an equivalent edge crack shown in Fig. 6. The required stress intensity factor and crack opening displacement solution to a single edge crack in a finite sheet subjected to segment uniform stress are given in the Appendix by using the weight function method (Wu and Carlsson, 1991). Using the superposition principle, the stress intensity factor and crack opening displacement of the equivalent edge crack can be obtained. The constraints of the single edge crack are zero crack opening displacement along the remaining elastic ligaments and no stress singularity at the crack tip. Subsequently, the plastic zone sizes and stress distribution in the ligaments can be obtained by solving the equations based on these constraints. The significance of treating the cracks, plastic zones and ligaments as a single edge crack as shown in Fig. 6 is that either the two cracks is symmetrical or asymmetrical, it can be analyzed by using the equivalent edge crack. However, for symmetrical collinear cracks, it is better to treat it as a single center crack to reduce the number of unknown variables. For instance, the stress distribution $\sigma_1(x)$ shown in Fig. 6 is redundant when the cracks are symmetrically distributed.

It is found that the present method is quite simple and versatile. The requirements of this method are the stress intensity factor and crack opening displacement solutions to a single crack subjected to uniform segment stress. These solutions are presented in the Appendix for a single center (edge) crack in finite and infinite

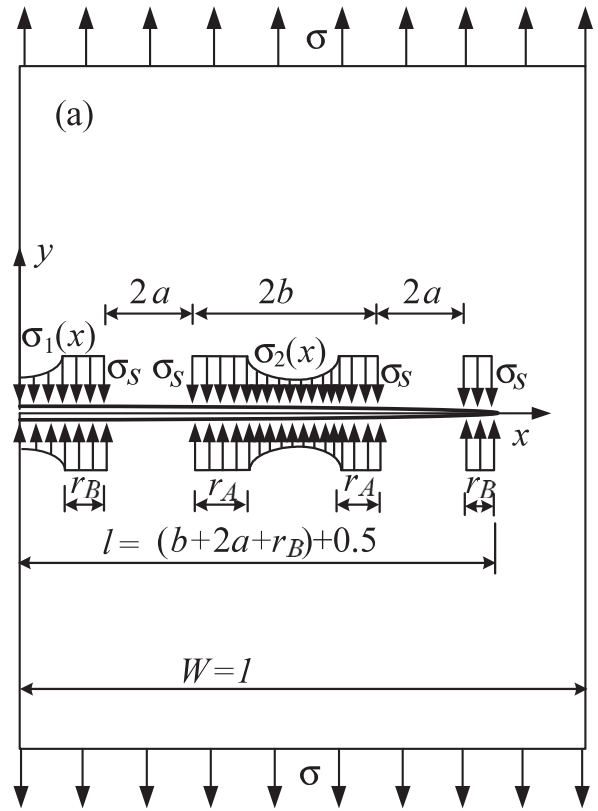


Fig. 6. An equivalent single crack to model the problem shown in Fig. 4(a).

plates. Using these solutions and the concept of the present method, the strip yield model for symmetric or asymmetrical collinear cracks in finite and infinite sheets can be solved. Besides the plastic zone sizes, the crack opening displacement and stress distribution along the ligament between cracks can be also obtained.

3.2. Application and verification by two collinear cracks

Two equal-length collinear cracks in infinite and finite sheets are used to verify the present method. The plastic zone sizes, crack (tip) opening displacements and stress distribution along the ligaments between the cracks are obtained and extensively compared with available analytical solutions and finite element results.

Firstly, two symmetrical equal-length collinear cracks in an infinite sheet (in Fig. 4(a), the sheet is infinite) are taken as an example to demonstrate the capability of the present method for collinear cracks in infinite elastic domain. Geometric sequences $q = \Delta x_i/x_{i-1}$ are used to model the elastic ligament $[0, X_1]$ shown in Fig. 4(b), where $\Delta x_i = x_i - x_{i-1}$, $i = 1, 2, 3 \dots N$. For a given common ratio q , N is increased until the corresponding obtained plastic zone sizes converge. For the present two cracks, $q = 0.96$ and $N = 80$ are used. The plastic zone sizes and stress distribution along the elastic ligament are determined by solving Eq. (9). The normalized plastic zone sizes for the crack tips A and B of three crack configurations $a/(a + b)$ -values subjected to various applied load are represented by the solid circles shown in Fig. 7(a) and (b), respectively. r_0 in Fig. 7 is the Dugdale plastic zone size for a single center crack in an infinite sheet. Having obtained the plastic zone sizes and stress distribution along the ligament between the cracks, the corresponding crack tip opening displacement for the crack tips A and B determined by using Eq. (8) are shown in Fig. 8(a) and (b), respectively. For comparison purpose, also shown in these figures are the results given by Collins and Cartwright (2001) and Xu

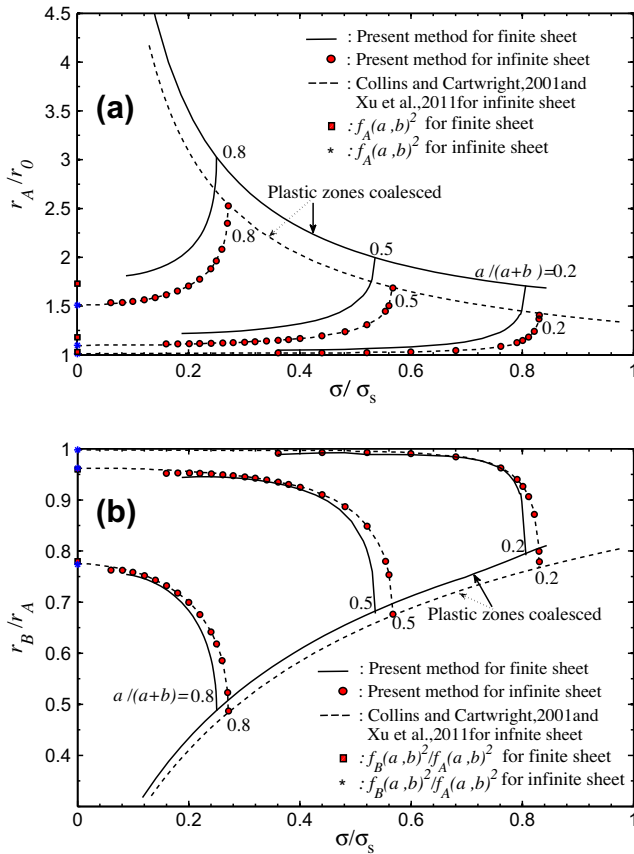


Fig. 7. Normalized plastic zone sizes as a function of applied stress σ/σ_s for various $a/(a+b)$ -values; $r_0 = a[\sec(0.5\pi\sigma/\sigma_s) - 1]$, $(2a+b)/w = 0.5$. (a) inner crack tip, (b) ratio of the plastic zone sizes between the outer and inner crack tips.

et al. (2011) based on complex stress function method and weight function method, respectively. Very good agreement is observed for $\sigma/\sigma_c \geq 1/3$, where σ_c is the plastic zone critical coalescence load for a given crack configuration by solving Eq. (10). When the applied load is less than $\sigma/\sigma_c < 1/3$, the plastic zone is very small and high stress gradient are observed in the elastic ligament. As a result, more segments are required to discretize the ligament to obtain high accurate results. However, for this case, the normalized plastic zone size and crack opening displacement are limited to the corresponding non-dimensional stress intensity factors f_A^2 and f_B^2 for a given crack configuration, which can be observed from Figs. 7 and 8. This tendency is also observed for three collinear cracks by Xu and Wu (2012) and in the following two equal-length cracks in finite sheet.

With the confidence gained from the two symmetrical collinear cracks in an infinite sheet, the present method is applied to analyze the strip yield model for the two cracks in a finite sheet. Once the code for collinear cracks in infinite sheet is available, it is easily extended to analyze collinear cracks in finite sheet. Using the stress intensity factor and crack opening displacement expression (Eqs. (A.7) and (A.4) in Appendix A) for a center crack in a finite width sheet, the plastic zone sizes and stress distribution along the elastic ligament can be determined by solving Eq. (9). The normalized plastic zone sizes for the crack tips A and B for various $a/(a+b)$ -values under $(2a+b)/w = 0.5$ (Fig. 4(a)) are represented by the solid lines shown in Fig. 7(a) and (b), respectively. The stress distribution $\sigma(x)$ in the ligament $[0, b]$, $b = a = 1/6$ denoted by the solid dot are shown in Fig. 9. The plastic zone size (r_A) are enlarged as the increase of the applied load and finally coalesced at $\sigma/\sigma_s = 0.5355$,

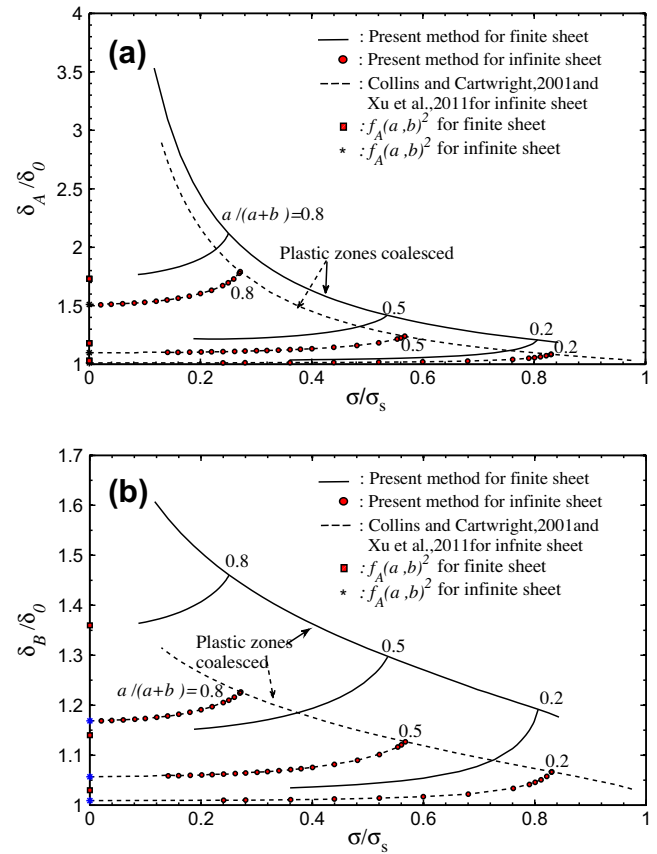


Fig. 8. Crack tip opening displacements as a function of applied stress σ/σ_s for various $a/(a+b)$ -values; $\delta_0 = 8a\sigma_s/(\pi E) \ln[\sec(0.5\pi\sigma/\sigma_s)]$, $(2a+b)/w = 0.5$. (a) inner crack tip, (b) outer crack tip.

see Fig. 9. High stress gradient are observed at relatively small load, for example $\sigma/\sigma_s = 0.2$. For even small applied load, very high stress gradient would occur. More segments are required to obtain accurate plastic zone size and stress distribution. Having obtained the plastic zone sizes and stress distribution along the ligament between the cracks, the corresponding crack opening displacement for the crack tips A and B determined by using Eqs. (8) and (12) are shown in Fig. 8(a) and (b), respectively. Also shown in Fig. 8 are the corresponding non-dimensional stress intensity factors square f_A^2 and f_B^2 which are determined by using Finite Element Method (FEM). It is also found from Fig. 8 that for $\sigma/\sigma_s < 1/3$, the normalized crack tip opening displacements for the crack tips A and B approach to f_A^2 and $f_B^2 \cdot (f_B^2/f_A^2)$, respectively. The crack opening profile can be also determined by using Eqs. (8) and (12). The solid dots in Fig. 10 shows the results for a given crack geometry $a = b = 1/6$ (Fig. 4(a)) under different applied loads. It is observed that for the critical case, $\sigma/\sigma_s = 0.5355$, the corresponding crack opening displacement at $x = 0$ is zero.

FEM is an alternative method to analyze the strip yield model for collinear cracks in finite sheet. Due to the symmetry of the problem shown in Fig. 4(a), only one quarter of the panel is modeled. The crack length in the finite element model is $2a + r_A + r_B$. Uniform yield compression stress σ_s and applied tension stress σ are applied at the plastic zones and the model edge, respectively. Proper symmetry boundary conditions are applied at the edge of the model. Very fine plane stress element mesh is created in the crack tip location and gradually transforms to large one. The element length at the crack tip is less than $\text{Min}[(2a + r_A + r_B)/100, r_B/10]$. The elastic analysis is carried out by using MSC/NASTRAN®

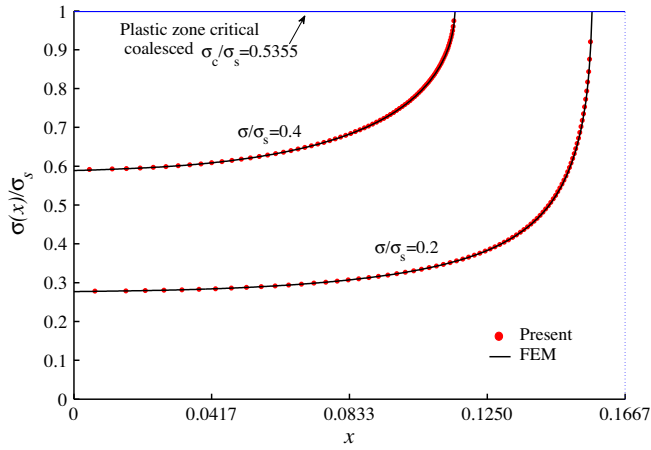


Fig. 9. Stress distribution along the ligament between cracks, $x \in [0, b]$, $a = b = 1/6$, see Fig. 4(a).

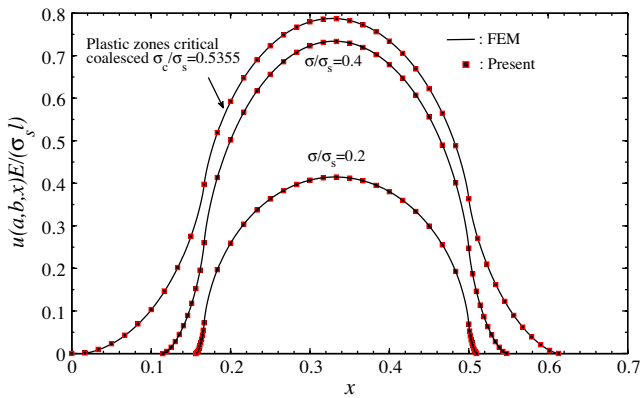


Fig. 10. Crack opening profiles for the strip yield model for two equal-length collinear cracks in a finite sheet shown in Fig. 4(a) with $a = b = 1/6$. Due to the symmetry of the problem, the results are given for one of the cracks.

software, and the Virtual Crack Closure Technique (VCCT) is used to determine the stress intensity factors. The unknown plastic zone sizes r_A and r_B are determined iteratively until the computed non-dimensional stress intensity factors are sufficient small (less than 0.01). The plastic zone sizes, stress distribution and the corresponding crack opening displacements for the strip yield model obtained by using FEM are also shown in Figs. 9 and 10. It is observed that the results obtained by the present method agree well with the FEM results. However, the present method is much more efficient than FEM.

From Figs. 7 and 8, quantitative finite width effect can be obtained when comparison are made between the finite and infinite width sheet for a given $a/(a+b)$ -value. It is observed that the finite width effect cannot be ignored.

More application and validation of the present method were given in the first author's thesis (Xu, 2012). For examples, the present method had been used to solve the strip yield models for two typical three symmetrical collinear cracks, a lead crack with two small cracks and three equal-length collinear cracks in infinite sheets. The plastic zone size and crack opening displacement were compared very well with those obtained by using the weight function method for multiple collinear cracks (Xu and Wu, 2012). Besides that, the strip yield model for two collinear cracks in a semi-infinite sheet was analyzed to demonstrate the capability of the present method for asymmetrical collinear cracks.

3.3. Practical application of the present method for MSD

The present unified method is shown to be simple, efficient and accurate. And it is found that the unknown variables, such as the ligament stress and plastic zones, will increase with the number of cracks. One limiting case is that infinite periodic equal-length collinear cracks are located in a sheet. It is difficult to use the present method to solve this problem. However, closed form solution to this case was given by Wu and Xu (2011). A common MSD problem is a lead crack with several small collinear cracks. Here, a lead crack with four small collinear cracks in a finite width sheet shown in Fig. 11(a) is used to illustrate the practical application of this method.

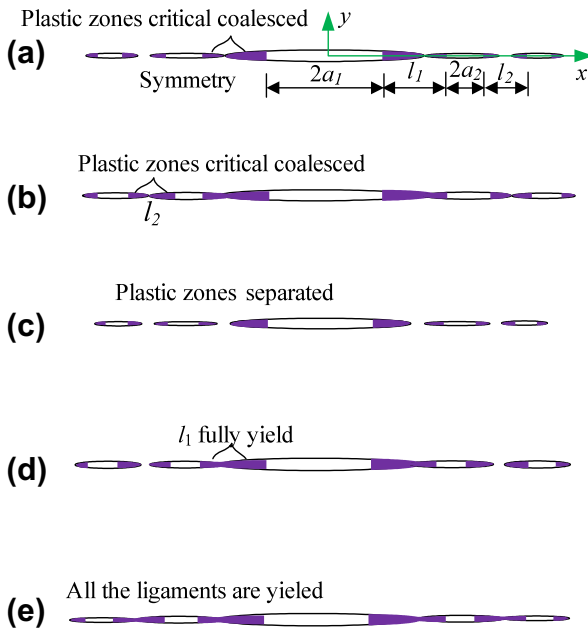
It is known from the present unified method introduced in Section 3.1 that the equation for the plastic zones coalescence and separated are different. As a result, for a given applied load, it needs to determine which equation is used to solve the plastic zone sizes and crack opening displacements. Five different strip yield models for the five collinear cracks are shown in Fig. 11. The plastic zones critical coalescence in the ligament l_1 and l_2 are shown in Fig. 11(a) and (b), respectively. The corresponding applied loads are defined as σ_{l1} and σ_{l2} , respectively. If the remote applied load σ is less than σ_{l1} ($\sigma < \sigma_{l1}$), all the plastic zones are separated as shown in Fig. 11(c). For $\sigma_{l1} < \sigma < \sigma_{l2}$, it means the ligament l_1 is fully yield, which is shown in Fig. 11(d). For $\sigma > \sigma_{l2}$, all the ligaments between the cracks are fully yield shown in Fig. 11(e).

The corresponding solution models are also given in Fig. 11. For simplicity, the determination of σ_{l1} is reduced to analyze the plastic zones critical coalescence of three collinear cracks. It is based on the observation that the outside small cracks have little influence on the plastic zone sizes of the center crack (Xu and Wu, 2012). In order to obtain the critical applied load for the three collinear cracks, the plastic zones and the cracks are modeled as a single crack. This equivalent single crack is subjected to remote uniform applied stress σ_{l1} and compressive yield stress σ_s applied at the plastic zones. The constraints of the equivalent single center crack are: the stress intensity factor and the minimum crack opening displacement in the ligament l_1 are zero. The weight function method is used to obtain the stress intensity factor and crack tip opening displacement for such complex loading case. The critical applied load σ_{l1} , plastic zone sizes and crack tip opening displacement δ_{l1} can be determined by solving the equations based on these constraints. The solution to the problem shown in Fig. 11(b) and (e) can be obtained by following the same way. The requirements for Fig. 11(b) are: the stress intensity factor and minimum crack opening displacement in ligament l_2 of the single crack equal to zero. Based on these requirements, the critical applied load, plastic zone sizes (r) and crack opening displacement can be determined. For Fig. 11(e), the plastic zone size r can be determined based on zero stress intensity factor for the single crack. More detailed analysis and validation of this method were given in Wu and Xu (2011).

The solutions to the problem shown in Fig. 11(a), (b) and (e) are relatively simple. However, when the stress distribution among the ligament is unknown, such as in the cases shown in Fig. 11(c) and (d), the unified method presented in Section 3.1 is applied to obtain the plastic zone size and crack opening displacement. In order to simplify the problem shown in Fig. 11(c), only the center three cracks are considered and subsequently solved by using the unified method.

Having obtained the plastic zone size and crack opening displacement, the crack growth criterion given in Eqs. (2) and (3) are used. Once the cracks grow, it becomes a new five crack configuration. This new five crack configuration needs to be re-evaluated by following the above way. As the crack grows, the ligament l_1 and l_2 will fracture successively. Accordingly, it reduces to a three and

Strip yield models for five collinear cracks



The corresponding solution models

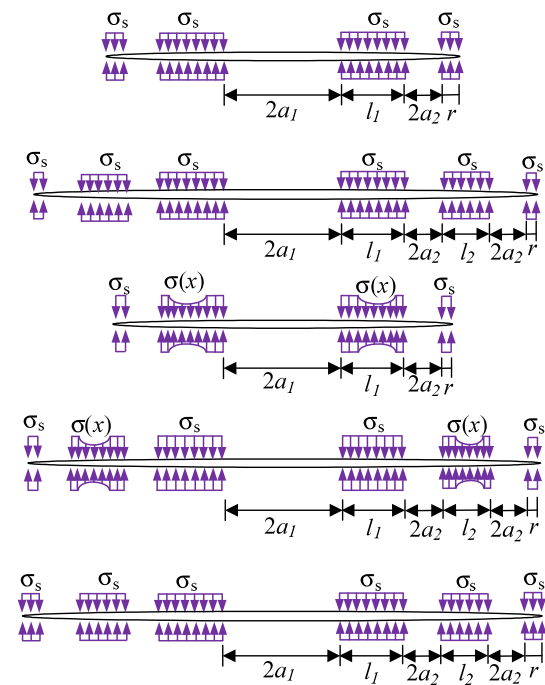


Fig. 11. Strip yield models for five collinear cracks in a finite sheet subjected to different loads.

further one crack growth problem. And, the codes for three and one crack growth will be used.

4. Experiment

The purpose of the experimental testing is two fold. One is coupon test to determine the basic material properties, and the other is residual strength test for sheet with MSD to verify the capability of the present method for predicting residual strength.

4.1. Specimens

The material for this investigation is aluminum alloy 2024-T3, which is widely used in aerospace structures. All the specimens used in this research are machined from the same lot sheet (3650 mm × 1200 mm × 1 mm) to avoid lot-to lot variation. The material L-T orientation is chosen, since it had smaller amount of tunneling once the crack began to grow than that of the T-L orientation (Sutton et al., 1995). The Stress-strain curve (L-T Direction) determined by following ASTM-E8 (2009) is shown in Fig. 12. The material properties are: yield strength $\sigma_{0.2} = 294.2$ Mpa, ultimate strength $\sigma_u = 429.8$ Mpa, elastic modulus $E = 68000$ Mpa and Poisson's ratio $\nu = 0.3$. The corresponding material properties supplied by ALCOA® are $\sigma_{0.2} = 293.5$ Mpa, $\sigma_u = 434.0$ Mpa, very good consistency is observed.

The compact-tension C(T) specimen is used to obtain the fracture parameters required in the crack growth prediction. It is difficult to manufacture a wide sheet with fatigued-precracked MSD, two types of C(T) specimen, cut-sawed notch and pre-fatigue cracked specimens, are designed to study the notch effect on the critical crack opening displacement and residual strength. Four specimens are used for each type. The notch is 0.2 mm in width and 150 mm in length. For the fatigued specimen, it is initially sawed at length 148 mm, then subjected to cyclic loading at $P_{\max} = 560$ N, $R = 0.06$ to let the notch grow 2 mm. Details of the

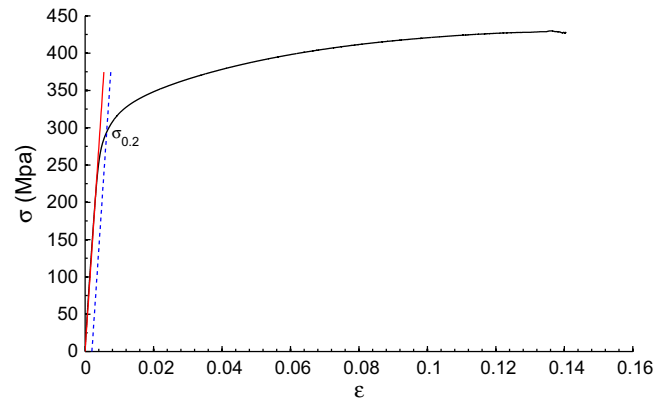


Fig. 12. Stress-strain curve for 2024-T3 sheet with 1 mm in thickness.

geometrical dimensions are designed according to ASTM standard E2472 (2007) and shown in Fig. 13.

In order to verify the capability of present method to predict the stable crack growth and residual strength for aluminum alloy sheet with MSD, a MSD test matrix including 32 specimens is designed. The specimen is 600 mm × 1140 mm in size. There are four types of MSD containing two, three, five and seven symmetrically collinear cracks shown in Fig. 14(a). All the cracks are made by saw cut. The notch width is the same as the sawed C(T) specimen. Fig. 14(b) shows the detailed geometrical dimension for a specimen with seven cracks. Details of geometrical dimensions of the four type crack configuration are listed in Table 1. The definition of each crack configuration MSDX- l_1 - l_2 - l_3 follows this rule: X represents the number of cracks; l_1 , l_2 and l_3 are the ligament lengths. It is observed from this table that some ligaments are very short, while some are relative long. The short ligament is designed to model the fracture of the ligament one by one. While the long ligament is designed for the sheet failed immediately at the fracture of ligament. In

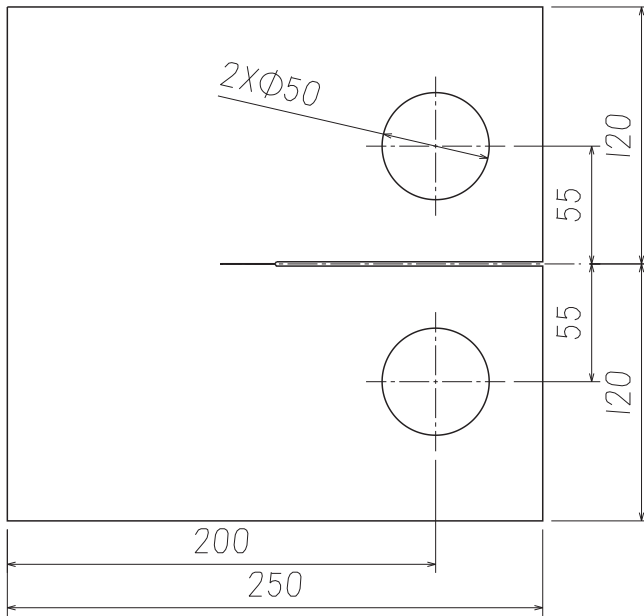


Fig. 13. Detailed geometrical dimensions of the C(T) specimen.

the residual strength test, two specimens are tested for each crack configuration. Since wide and thin specimen will experience out of plane displacements along the crack flanks, guide plates are used to restrict the buckling in all these specimens.

4.2. CTOA measurement and residual strength test

The CTOA is defined as the angle made by two straight lines; one line contains the crack tip and a point on the upper crack surface, the other contains the crack tip and a point on the lower crack surface. As a result, the CTOA is a function of the distance between the point and crack tip. The CTOA is a local fracture parameter, but the distance cannot be less than 0.25 mm. It is because the measurement technique is unable to resolve CTOA at such a distance. The distance was recommended to be 0.5–1.5 mm in ASTM standard E2472. Fig. 15 shows a typical crack tip opening angle at 1 mm behind the crack tip. The Optical Microscopy (OM) method is used to measure the CTOA. The setups for this method include (a) a long focus length microscope, Moritex® MML1-HR65DVI-5 M, its maximum horizontal field of view is 8 mm. It means that for most MSD configurations, only one crack tip is observed; (b) a video camera with resolution of 2448×2050 pixels to obtain images of the tearing crack; (c) a video recorder to store the images; and (d) a PC with both monitor and software to precisely

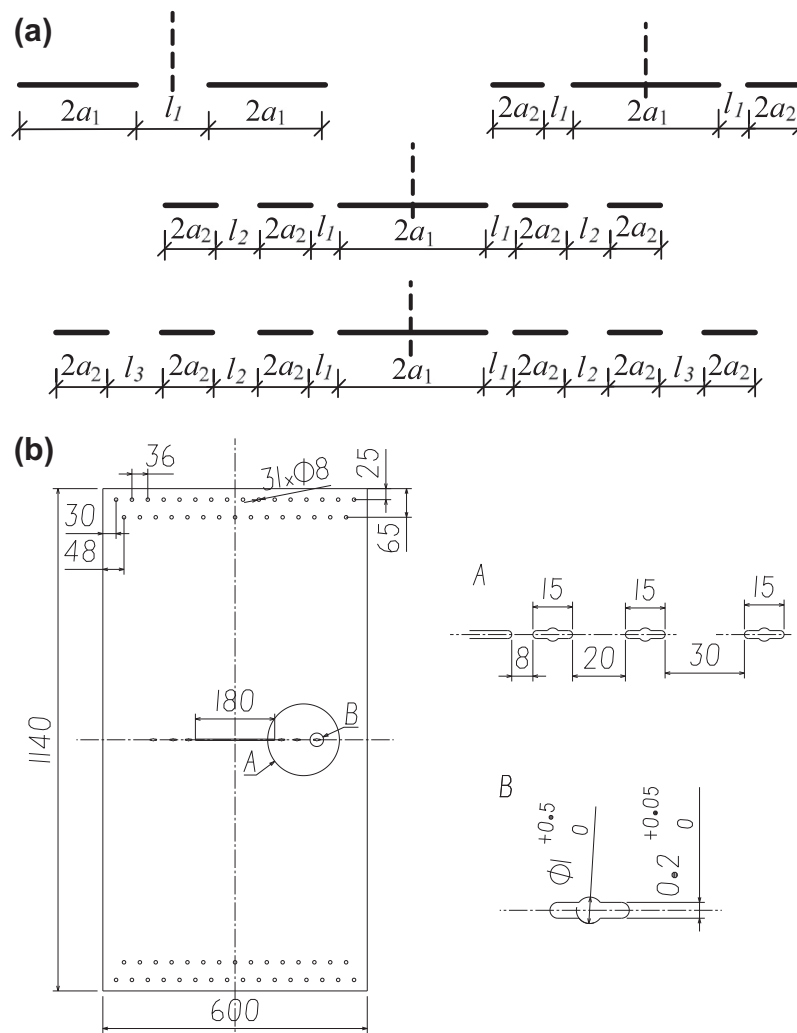


Fig. 14. Geometry dimensions of MSD specimen. (a) Four types of MSD configurations, (b) Detailed geometrical dimensions for MSD7_8_20_30.

Table 1
Detailed geometrical configurations of various MSD sheets.

Specimen ID	$2a_1(\text{mm})$	$l_1(\text{mm})$	$l_2(\text{mm})$	$l_3(\text{mm})$	$2a_2(\text{mm})$	Number
MSD2_08	120	8				2
MSD2_12	120	12				2
MSD2_18	120	18				2
MSD3_08	180	8			15	2
MSD3_12	180	12			15	2
MSD3_18	180	18			15	2
MSD5_6_10	180	6	10		15	2
MSD5_6_15	180	6	15		15	2
MSD5_8_15	180	8	15		15	2
MSD5_8_20	180	8	20		15	2
MSD5_15_60	120	15	60		15	2
MSD7_6_10_20	180	6	10	20	15	2
MSD7_6_12_30	180	6	12	30	15	2
MSD7_8_15_20	180	8	15	20	15	2
MSD7_8_20_30	180	8	20	30	15	2
MSD7_30_60_30	120	30	60	30	15	2

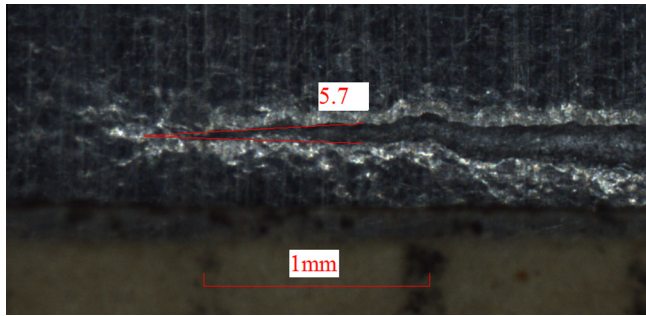


Fig. 15. Measurement of crack tip opening angle.

control (0.001 mm in the present test) the three-dimensional position of the long focal-length microscope and also to analyze the image to obtain CTOA. The transverse magnification of the microscope is approximately 300 pixels per millimeter. Fig. 15 shows a typical image obtained by using the above setups. More detailed information about the experiment was given in the first author's thesis (Xu, 2012).

Another important parameter is the current crack length during the crack tearing. There are many methods used for the measurement of crack length. However, most of them are valid for single crack problem. In the present study, the OM method is applied to measure the crack length for all the cracked specimens. It is possible to use one set of equipment to measure all of the crack growth for MSD specimen. But it is time-consuming, complex and error-prone. For MSD specimen, the information for one crack tip is measured. Initially, the crack tip at the lead crack is selected. All the tests are performed in displacement control. The test will be terminated immediately once the ligaments link up. Subsequently, the video camera and the long focal-length microscope are moved to the new created lead crack tip. After everything is well, the test will be continued until the break of the entire sheet.

Using the above method and setups, the CTOA obtained from C(T) specimens are given in Fig. 16. It is observed that larger CTOA is required for crack initiation for sawed crack specimen than that of fatigued specimen. However, after about 2 mm stable crack tearing, the difference of crack growth behaviors between sawed and fatigued cracks is ignorable. The average residual strength for the sawed and fatigued C(T) specimen are 4295 N and 4302 N with the coefficient of variation of 0.015 and 0.008, respectively. For comparison purpose, the load against crack extension results for

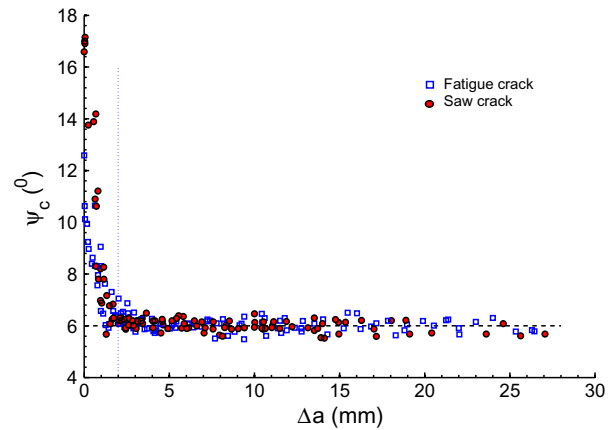


Fig. 16. Crack tip opening angle against crack extension of C(T) specimen, $(\varphi-\Delta a)$.

C(T) and MSD specimen will be given in Section 5 to verify the predicted results.

5. Residual strength prediction and validation

5.1. Parameter determination

The critical crack initiation parameter and critical constant CTOA α_c should be determined before the stable crack growth analysis for sheets with MSD. However, they were not directly obtained from the experimental measurement (Galatolo and Nilsson, 2001). The reason can be analyzed from the experiment and the analytical model. Experimentally, the crack initiation value δ_0 is associated with complex three dimensional process and it is very difficult to define and measure it. For the constant critical opening angle, it is measured from the specimen surface. Experimental and numerical analysis results (Newman et al., 2003a,b) had shown that the crack opening angle was smaller at the inner plate than that at surface α_{surf} . Analytically, the three dimensional process at the crack tip during tearing cannot be considered in the plane stress strip yield model. Another important factor may be due to the fact that the strip yield model is a simple model after all. It is hard to exactly describe the elastic–plastic displacement field of a stable growth crack. As a result, a correction is required. A plane stress constraint effect factor SF was proposed to consider the three dimensions effect by Galatolo and Nilsson (2001).

$$\alpha = SF \cdot \alpha_{surf} \quad (13)$$

In practice, a pair of 'optimal' δ_0 and α_c is selected as the critical values. Using the 'optimal' values, the predicted crack growth behaviors of coupon specimens agree very well with the corresponding experiment observations. Since the MSD is made by saw cut, the saw cut C(T) specimen is used to determine these critical values. The weight function method (Wu and Carlsson, 1991) is used to determine the crack opening displacement for crack growth analysis.

The crack extension against load of fatigued and sawed C(T) specimens are given in Fig. 17. Some difference in the crack growth behaviors of the sawed and fatigued cracks are observed when the crack growth length $\Delta a \leq 5$ mm. It implies that if the crack growth amount of each crack in the ligament is less than 5 mm, there must be some difference between the fatigued and sawed MSD. However, after about 5 mm growth, the crack growth behaviors are quite the same. And the maximum residual strengths of the sawed and fatigued specimen are nearly the same when the variation of the experiment is considered. It is also observed that the maximum

residual strengths of the sheet with MSD are occurred when the crack have grown much more than 5 mm. As a result, the maximum residual strength of the present saw MSD is considered to be equivalent to that of fatigued MSD.

Since it is difficult to make a wide sheet with fatigue-precracked MSD, in the present study, the sawed C(T) specimen is used to obtain the critical crack initiation displacement δ_0 and critical CTOA α_c to apply and verify the present method for crack growth analysis of sheets with sawed MSD. Following the flow chart given in Fig. 3, Fig. 17 shows the predicted load-crack extension curves obtained by four different pairs of parameters. It is observed that the predicted result obtained by the parameters $\delta_0 = 0.13$ mm and $\alpha_c = 3.4^\circ$ agrees well with the test data of the saw-cut C(T) specimen. Therefore, these values ($\delta_0 = 0.13$ mm and $\alpha_c = 3.4^\circ$) are used as critical material properties to predict crack growth for MSD specimens.

5.2. Experimental and predicted crack growth behaviors

Following the method described in Sections 2 and 3 and using the critical values $\delta_0 = 0.13$ mm and $\alpha_c = 3.4^\circ$, the predicted crack growth process for sheets with two, three, five and seven collinear cracks are given as follows. For comparison purpose, the corresponding experimental results are also presented.

5.2.1. Two collinear crack configurations

The MSD2 has three different crack configurations. The difference between these crack configurations is the ligaments length between the cracks. In order to verify the capability of present method to predict the crack growth behavior after the fracture of ligament, all ligaments are designed to be relatively short.

At the beginning, the unified method is used to solve the strip yield model. As the increase of the applied load, the crack will grow and the ligament will fracture. After the fracture of the ligament, a lead new center crack is formed. Using the weight function for a center single crack, the program for the C(T) specimen can be modified to analyze this case. An example of the predicted crack growth process (solid lines) is shown in Fig. 18. For comparison purpose, the symbols shown in this figure are the corresponding experimental data (each crack configuration has two test specimens). It is observed that the predicted results are in good agreement with the test results.

5.2.2. Three collinear crack configurations

The three crack configuration is quite different from the two crack configuration. The center crack is much longer than that

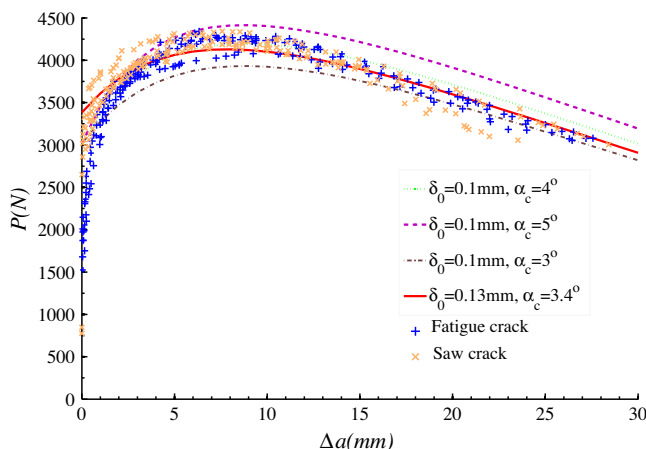


Fig. 17. Crack extension against load of C(T) specimen (Δa - P curve).

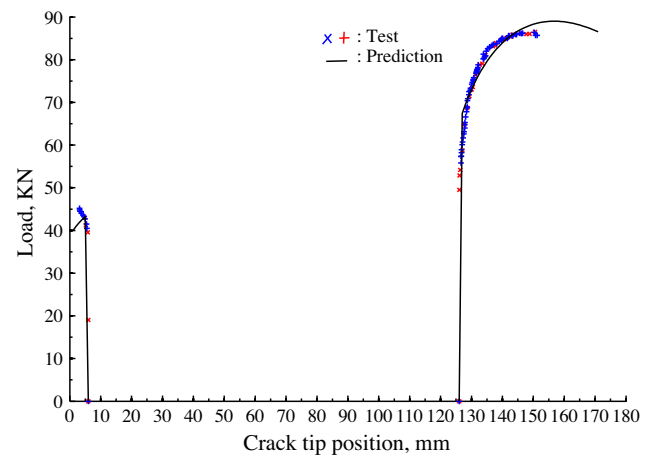


Fig. 18. Experimental and predicted Δa - P curve of MSD2-12 specimen.

of the side cracks. However, the analysis process is nearly identical with that of the two crack configuration. In Fig. 19 shows an example of predicted and experimental crack growth against applied load curves. Due to the limitation of experiment method used in the study (Section 4.2), the experimental crack growth information for the original crack tip at $x = 102$ mm is unavailable.

5.2.3. Five collinear crack configurations

The MSD5 specimen is designed to carry load after the fracture of ligament l_1 . It is observed from Table 1 that the ligament l_1 is relative short. However, for the ligament l_2 , it is much longer than that of l_1 , especially the MSD5-15-60 specimen ($l_2 = 60$ mm). Two distinct fracture scenarios are shown in Figs. 20 and 21 as examples. For the MSD5-6-15 specimen (as well as MSD5_6_10, MSD5_8_15 and MSD5_8_20), the experimental and predicted maximum residual strengths are occurred after the fracture of all the ligaments. While, the specimen MSD5-15-60 is broken down immediately at the fracture of ligament l_2 . Since the quick fracture of this specimen, the crack growth information for the outside crack tip is not recorded. However, the predicted result is able to describe the entire crack growth process, see the solid lines in Fig. 21. After the applied load reaches the maximum residual strength 95.5KN, unstable crack growths are observed from the crack tips, which result in the fracture of the whole sheet.

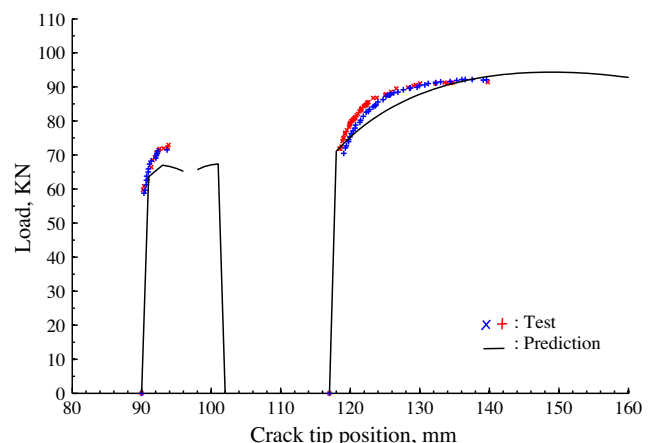


Fig. 19. Experimental and predicted Δa - P curve of MSD3-12 specimen.

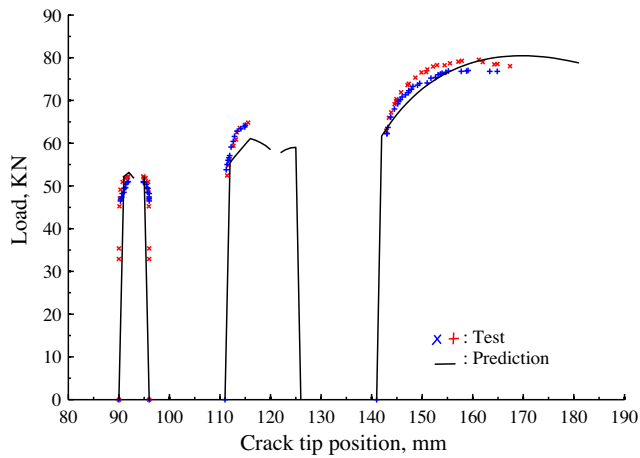


Fig. 20. Experimental and predicted Δa - P curve of MSD5-6-15 specimen.

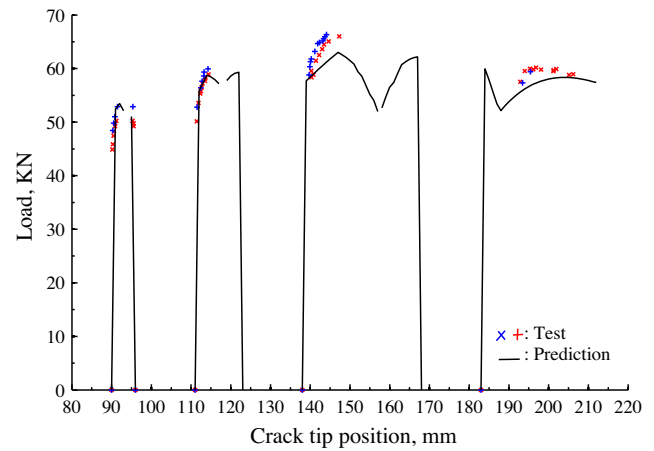


Fig. 23. Experimental and predicted Δa - P curve of MSD7_6_12_30 specimen.

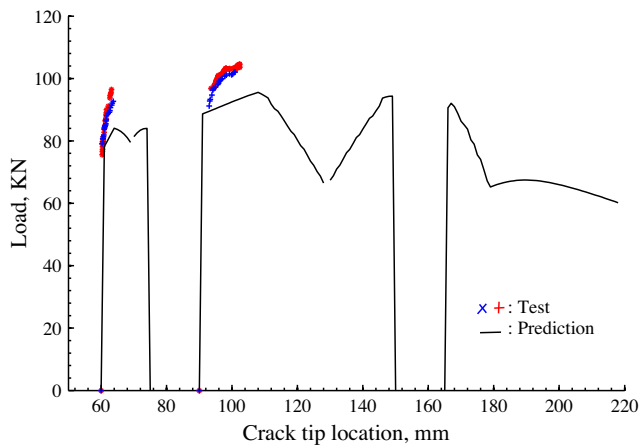


Fig. 21. Experimental and predicted Δa - P curve of MSD5-15-60 specimen.

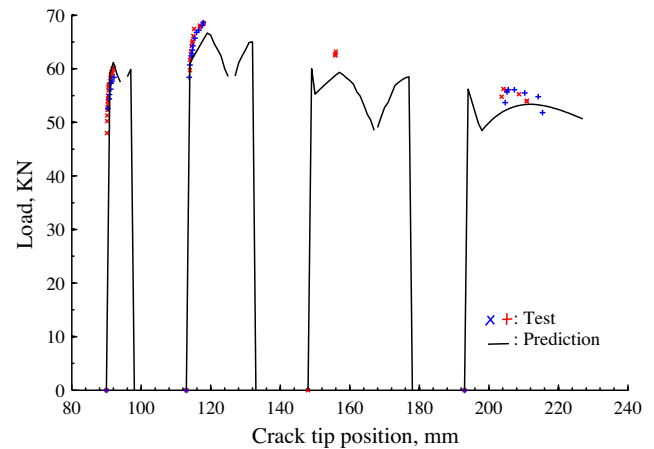


Fig. 24. Experimental and predicted Δa - P curve of MSD7_8_20_30 specimen.

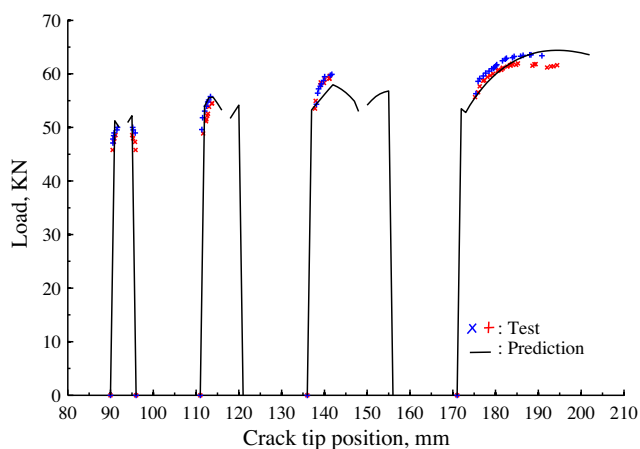


Fig. 22. Experimental and predicted Δa - P curve of MSD7_6_10_20 specimen.

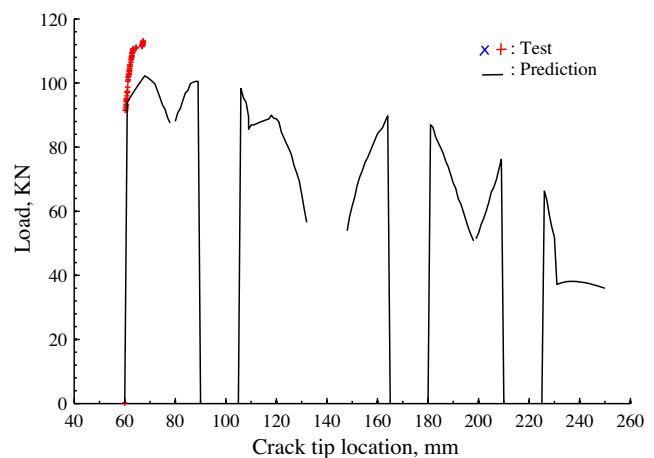


Fig. 25. Experimental and predicted Δa - P curve of MSD7-30-60-30 specimen.

5.2.4. Seven collinear crack configurations

The most complex and interesting crack configuration is the seven crack configuration. Various fracture scenarios can be observed from this test. The maximum residual strength is occurred after the fracture of all ligaments shown in Fig. 22. In Figs. 23 and 24, the

maximum residual strengths are appeared at the fracture of ligament l_3 and l_2 , respectively. The worst case shown in Fig. 25 is that the fracture of ligament l_1 ($l_1 = 30$ mm) results in the break of the entire sheet. And again, the predicted results shown in these figures are compared well with the corresponding test datum.

Table 2

Experimental and predicted residual strengths for sheets with various MSD.

Specimen ID	Test (KN)				Prediction (KN)				Error (%)			
	Pl_1	Pl_2	Pl_3	P_{max}	Pl_1	Pl_2	Pl_3	P_{max}	Pl_1	Pl_2	Pl_3	P_{max}
MSD2_08	38			86.8	37.3			90.2	−1.8			3.9
MSD2_12	45.5			86.3	43.2			89	−5.1			3.1
MSD2_18	55.9			85.3	50.7			87.3	−9.3			2.3
MSD3_08	64.1			94	61.5			96.8	−4.1			3.0
MSD3_12	72.5			92	67.4			94.3	−7.0			2.5
MSD3_18	79.2			89.2	74.4			90.8	−6.1			1.8
MSD5_6_10	54.4	61.8		82	50.2	54.6		83.3	−7.7	−11.7		1.6
MSD5_6_15	52	64.7		78.5	53.2	61.1		80.5	2.3	−5.6		2.5
MSD5_8_15	60.8	68		78.6	56.5	60.3		79.4	−7.1	−11.3		1.0
MSD5_8_20	61.2	71.8		76.4	59.1	64.3		76.6	−3.4	−10.4		0.3
MSD5_15_60	94.5	103.3		103.3	84.1	95.5		95.5	−11.0	−7.6		−7.6
MSD7_6_10_20	49.4	55.3	59.4	62.8	52.2	57.1	58	64.4	5.7	3.3	−2.4	2.5
MSD7_6_12_30	51.4	59.9	66.4	66.4	53.5	59.3	63	63	4.1	−1.0	−5.1	−5.1
MSD7_8_15_20	58.5	62.4	60	62.4	57.7	60.2	55.5	60.8	−1.4	−3.5	−7.5	−2.6
MSD7_8_20_30	59.5	68.4	64	68.4	61.5	66.7	59.4	66.7	3.4	−2.5	−7.2	−2.5
MSD7_30_60_30	112	–	–	112	102.3	–	–	102.3	−8.7	–	–	−8.7

5.3. Summary and comparisons

By proper design of MSD geometries, various fracture scenarios are achieved. The scatter of the experimental data is within 5% for each type of cracked configuration. Table 2 lists the experimental and predicted ligament fracture loads (Pl_i) and maximum residual strengths (P_{max}). The experimental result shown in Table 2 is the average value of the two test specimens for a given crack configuration. It is observed that the maximum error in the ligament fracture load is −11.7%, and the predicted residual strengths are within 9% of the experimental results.

Elastic–plastic FEM is an alternative widely used method to predict the residual strength for cracked structures. In order to model the complex three dimensional displacement fields at the crack tip, Dawicke and Newman (1998) used a three dimensional elastic–plastic finite element analysis combination with CTOA criterion to predict residual strength for panels with single and multiple site cracks. The predicted results were within 7% of the experimental results. Considering the complex modeling and computation demand of the three-dimensional finite element analysis, Newman et al. (2003a,b) and Seshadri et al. (2003) proposed two dimensional finite elements with a “plane strain core” to model the high-constraint condition around the crack front. The predicted residual strengths for stiffened and unstiffened wide panels were compared well with the corresponding test results. Using the “plane strain core” model and CTOD criterion embedded in ABAQUS®, the ligament fracture loads and residual strengths for some of the present MSD configurations were recently given by Huang et al. (2013). It was found that the predicted residuals strength by using FEM were within 11% of the test results. However, the computational and modeling demands are quite different. For a given MSD configuration, it takes at least two hours (a computer with a Pentium® Dual-Core CPU E5300@2.60 GHz and 3.00 GB RAM) to complete a residual strength prediction by using FEM. And, it does not include the time for creating the finite element model. In order to model the crack growth, the “debond” technique in ABAQUS® is used. The finite element method involves material and contact non-linear analysis. Rich experiences on finite element modeling and analysis are required. However, for most of the present MSD configuration, two minutes is enough to complete a residual strength analysis by using the present method. Furthermore, once the crack growth analysis program for a given crack config-

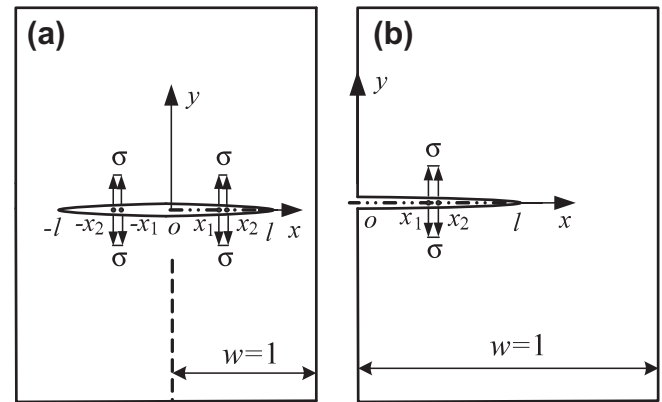


Fig. A.1. A crack in a finite sheet subjected to segment uniform stress. (a) a center crack; (b) an edge crack.

uration is available, there is no modeling time. These advantages are very useful for parameter analysis.

6. Conclusions

A unified method for solving the strip yield model for collinear cracks in finite and infinite sheets is proposed. The method is based on the weight function of a single crack. Two equal-length collinear cracks are used to apply and verify this method. Combined with the CTOA criterion, the unified method is used to predict the crack growth behavior and residual strength for flat sheet made of 2024-T3 aluminum alloy with various multiple site damage. In order to verify the present method, experiments are designed and tested. The experiment includes basic material properties determination and residual strength tests for four types of multiple site crack configurations in finite sheets. By proper design of MSD geometries, various fracture scenarios are achieved. The experimental results provide important information for assessing the present method. Key finding of the present research are given as follows:

- (1) The present unified method is simple, efficient, accurate and versatile for solving the strip yield model for collinear cracks in finite and infinite width sheets.

- (2) This unified method combined with CTOA criterion is able to predict the stable crack growth behaviors well for the present sheets with MSD. The predicted residual strengths are within 9% of the corresponding experimental results. Compared to finite element method, the present method is much more efficient.
- (3) The present experimental crack growth results are valuable to verify other residual strength prediction method.

Acknowledgments

The first author is grateful for the financial support from Shanghai Jiao Tong University Grant Z-010-011. All the authors appreciate the reviewers' valuable comments.

Appendix A

Fig. A.1 shows cracks subjected to segment uniform pressure over the crack surfaces. The corresponding crack opening displacement and stress intensity factor solutions to a crack in finite and infinite width sheets are given as follows.

A.1. A center crack in an infinite sheet

The crack opening displacement is (Tada et al., 2000)

$$u(l, x_1, x_2, x) = \frac{2}{\pi E'} \left\{ (x_2 - x) \cosh^{-1} \left[\frac{(l - x_2)x + x_2 l}{l|x - x_2|} \right] - (x_1 - x) \cosh^{-1} \left[\frac{(l - x_1)x + x_1 l}{l|x - x_1|} \right] + \sin^{-1}[(x_2 - l)/l] - \sin^{-1}[(x_1 - l)/l] \right\} \cdot \sqrt{2lx - x^2} \quad (\text{A.1})$$

where $E' = E$ (plane stress), $E' = E/(1 - \nu^2)$ (plane strain). E is Young's modulus and ν is Poisson's ratio. The corresponding non-dimensional stress intensity factors for the left and right crack tips shown in Fig. 5(c) (The width is infinite) denoted by $f_L(l, x_1, x_2)$ and $f_R(l, x_1, x_2)$, respectively, are

$$f_L(l, x_1, x_2) = \frac{1}{\pi} \left\{ \sin^{-1}[(x_2 - l)/l] - \sin^{-1}[(x_1 - l)/l] + \left[\sqrt{2lx_2 - x_2^2} - \sqrt{2lx_1 - x_1^2} \right] / l \right\} \quad (\text{A.2})$$

$$f_R(l, x_1, x_2) = \frac{1}{\pi} \left\{ \sin^{-1}[(x_2 - l)/l] - \sin^{-1}[(x_1 - l)/l] - \left[\sqrt{2lx_2 - x_2^2} - \sqrt{2lx_1 - x_1^2} \right] / l \right\} \quad (\text{A.3})$$

A.2. A center crack in a finite width sheet

The crack opening displacement for a center crack subjected to symmetrically uniform loading over the crack surface $\pm[x_1, x_2]$ shown in Fig. A.1(a) was calculated by using the weight function method (Wu and Carlsson, 1991):

$$u_c(l, x_1, x_2, x) = 1/E' \cdot \int_{a_1}^l f_c(s, x_1) \sum_{i=1}^3 \beta_i(s) \cdot [1 - (x/s)^2]^{i-1.5} \cdot ds - 1/E' \cdot \int_{a_2}^l f_c(s, x_2) \sum_{i=1}^3 \beta_i(s) \cdot [1 - (x/s)^2]^{i-1.5} \cdot ds \quad (\text{A.4})$$

where $a_1 = \max(x_1, x)$ and $a_2 = \max(x_2, x)$, s is integral variable, and

$$f_c(s, d) = 1/\pi \cdot \sum_{i=1}^3 \beta_i(s) \cdot Q_i(d/s)$$

$$Q_1(d/s) = \cos^{-1}(d/s)$$

$$Q_i(d/s) = 1/(2i - 2) \cdot \{(2i - 3) \cdot Q_{i-1}(d/s) - d/s \cdot [1 - (d/s)^2]^{i-1.5}\}, \quad i \geq 2 \quad (\text{A.5})$$

The formulas for $\beta_i(s)$, $i = 2, 3$ ($\beta_1(s) = 2.0$) are

$$\begin{cases} \text{for } s \leq 0.5 \\ \beta_2(s) = \pi s/2 \cdot \tan(\pi s/2) \\ \beta_3(s) = 0 \\ \text{for } s > 0.5 \\ \beta_2(s) = -46.5 + 394.0s - 1332.2s^2 + 2264.0s^3 - 1926.3s^4 + 663.8s^5 \\ \beta_3(s) = 31.9 - 269.1s + 907.1s^2 - 1529.5s^3 + 1291.8s^4 - 438.9s^5 \end{cases} \quad (\text{A.6})$$

And, the non-dimensional stress intensity factor is:

$$f_c(l, x_1, x_2) = f_c(l, x_1) - f_c(l, x_2) \quad (\text{A.7})$$

The accuracy of the crack opening displacement and stress intensity factor are better than 1% for $l \leq 0.8$.

A.3. An edge crack in a finite width sheet

The crack opening displacement for Fig. A.1(b) was calculated by using the weight function method (Wu and Carlsson, 1991):

$$u_e(l, x_1, x_2, x) = 1/(E'\sqrt{2}) \cdot \int_{a_1}^l f_e(s, x_1) \cdot \sum_{i=1}^5 \beta_i(s) \cdot (1 - x/s)^{i-1.5} \cdot ds - 1/(E'\sqrt{2}) \cdot \int_{a_2}^l f_e(s, x_2) \cdot \sum_{i=1}^5 \beta_i(s) \cdot (1 - x/s)^{i-1.5} \cdot ds \quad (\text{A.8})$$

where $a_1 = \max(x_1, x)$ and $a_2 = \max(x_2, x)$, and

$$f_e(s, d) = \sqrt{2}/\pi \cdot \sum_{i=1}^5 1/(2i - 1) \cdot \beta_i(s) \cdot (1 - d/s)^{i-0.5} \quad (\text{A.9})$$

And the corresponding non-dimensional stress intensity factor is:

$$f_e(l, x_1, x_2) = f_e(l, x_1) - f_e(l, x_2) \quad (\text{A.10})$$

The formulas for $\beta_i(s)$ ($i = 1, 2, 3, 4, 5$) of an edge crack in a finite panel were given in Wu and Carlsson (1991).

References

- ASTM International, 2007. ASTM E2472-06 Standard test method for determination of resistance to stable crack extension under low constraint conditions.
- ASTM International, 2009. ASTM E8/E8M-09 Standard test methods for tension testing of metallic materials.
- Cherry, M.C., Mall, S., Heinemann, B., Grandt Jr, A.F., 1997. Residual strength of unstiffened aluminum panels with multiple site damage. *Eng. Fract. Mech.* 57 (6), 701–713.
- Chen, Y.Z., Wang, Z.X., 2012. Solution of multiple crack problem in a finite plate using coupled integral equations. *Int. J. Solids Struct.* 49, 87–94.
- Collins, R.A., Cartwright, D.J., 2001. An analytical solution for two equal-length collinear strip yield cracks. *Eng. Fract. Mech.* 68, 915–924.
- Dawicke, D.S., Newman Jr, J.C., 1998. Residual strength predictions for multiple site damage cracking using a three-dimensional finite element analysis and a CTOA criterion. In: Panontin, T.L., Sheppard, S.D. (Eds.), *Fatigue and Fracture Mechanics*, ASTM STP 1332, vol. 29. American Society for Testing and Materials.
- Deng, X.Y., Hutchinson, J.W., 1996. Approximate methods for analyzing the growth of large cracks in fatigue damaged aircraft sheet material and lap joints. *Finite Elem. Anal. Des.* 23, 101–114.
- Dugdale, D.S., 1960. Yielding of steel sheets containing slits. *J. Mech. Phys. Solids* 8, 100–104.
- FAA, 2010. Aging airplane program, widespread fatigue damage. Federal Register Rules Regul. 75 (219), 69746–69789.
- Fett, T., Munz, D., 1997. Stress intensity factors and weight functions, first ed. Computational Mechanics Publications, Southampton UK and Boston, USA.
- Galatolo, R., Nilsson, K.F., 2001. An experimental and numerical analysis of residual strength of butt-joints panels with multiple site damage. *Eng. Fract. Mech.* 68 (13), 1437–1461.

- Hsu, C.L., James, L., Yu, J., Lee, X.G., Paul, T., 2003. Residual strength analysis using CTOA criteria for fuselage structures containing multiple site damage. *Eng. Fract. Mech.* 70, 525–545.
- Huang, X.L., Zhang, X.J., Bai, G.J., Xu, W., Wang, H., 2013. Residual strength analysis of thin-walled structures with multiple site damage based on crack tip opening angle method. *J. Shanghai Jiaotong Univ.* 47 (4), 519–524.
- Jeong, D.Y., Brewer, J.C., 1995. On the linkup of multiple cracks. *Eng. Fract. Mech.* 51 (2), 233–238.
- Kuang, J.H., Chen, C.K., 2000. Use of strip yield approach for multiple-site damage failure scenarios. *J. Aircraft* 37 (5), 887–891.
- Labeas, G., Diamantakos, J., Kermanidis, Th., 2005. Crack link-up for multiple site damage using an energy density approach. *Theor. Appl. Fract. Mech.* 43, 233–243.
- Ma, Y., Omori, L., Okada, H., Atluri, S.N., Kobayashi, A.S., Tan, P., 1996. The T^* -integral analysis of aluminum panels. *Theor. Appl. Fract. Mech.* 4, 89–94.
- Mahmoud, S., Lease, K., 2004. Two-dimensional and three-dimensional finite element analysis of critical crack tip opening angle in 2024-T351 aluminum alloy at four thicknesses. *Eng. Fract. Mech.* 71, 1379–1391.
- Moukawsher, E.J., Heinemann, M.B., Grandt Jr, A.F., 1996. Residual strength of panels with multiple site damage. *J. Aircraft* 33 (5), 1014–1021.
- Newman, J.C. Jr., 1986. Evaluation of the crack tip opening displacement (VR) resistance curve method. In: Schwable, K.H. (Ed.), *The Crack Tip Opening Displacement in Elastic–Plastic Fracture Mechanics*, pp.157–176.
- Newman Jr, J.C., Dawicke, D.S., Seshadri, B.R., 2003a. Residual strength analyses of stiffened and un-stiffened panels – Part I. Laboratory panels. *Eng. Fract. Mech.* 70, 493–507.
- Newman Jr, J.C., James, M.A., Zerbst, U., 2003b. A review of the CTOA/CTOD fracture criterion. *Eng. Fract. Mech.* 70 (3–4), 371–385.
- Nilsson, K.F., Hutchinson, J.W., 1994. Interaction between a major crack and small crack damage in aircraft sheet material. *Int. J. Solids Struct.* 31 (17), 2331–2346.
- Nilsson, K.F., 1999. Influence of MSD crack pattern on the residual strength of flat stiffened panels. *Comput. Mech.* 23 (1), 39–52.
- Nishimura, T., 2002. Strip yield analysis of two collinear unequal cracks in an infinite sheet. *Eng. Fract. Mech.* 69, 1173–1191.
- Seshadri, B.R., Newman Jr, J.C., Dawicke, D.S., 2003. Residual strength analyses of stiffened and un-stiffened panels – Part II. Wide panels. *Eng. Fract. Mech.* 70, 509–524.
- Smith, B.L., Hijazi, A.L., Haque, A.K.M., Myose, R.Y., 2001. Strength of stiffened 2024-T3 aluminum panels with multiple site damage. *J. Aircraft* 38 (4), 764–768.
- Sutton, M.A., Dawicke, D.S., Newman Jr, J.C., 1995. Orientation effects on the measurement and analysis of critical CTOA in an aluminum alloy sheet. In: *Fracture Mechanics. ASTM STP 1256*, vol. 26, pp. 243–255.
- Swift, T., 1994. Damage tolerance capability. *Int. J. Fatigue* 16 (1), 75–96.
- Tada, H., Paris, P.C., Irwin, G.R., 2000. *The Stress Analysis of Cracks Handbook*, third ed. ASME Press, New York.
- Wang, L., Brust, F.W., Atluri, S.N., 1997. The elastic-plastic finite element alternating method (EPFEAM) and the prediction of fracture under WFD conditions in aircraft structures. *Comput. Mech.* 20 (3), 199–212.
- Wu, X.R., Carlsson, A.J., 1991. *Weight Functions and Stress Intensity Factor Solutions*, first ed. Pergamon Press, Oxford.
- Wu, X.R., Xu, W., 2011. Strip yield cracks analysis for multiple site damage in infinite and finite panels – a weight function approach. *Eng. Fract. Mech.* 78 (14), 2585–2596.
- Xu, W., 2012. Weight function method for aircraft structure multiple site damage analyses and residual strength prediction, Ph.D. Thesis. Shanghai, Shanghai Jiao Tong University (in Chinese).
- Xu, W., Wu, X.R., Wang, H., 2011. Weight functions and strip yield solution for two equal-length collinear cracks in an infinite sheet. *Eng. Fract. Mech.* 78 (11), 2356–2368.
- Xu, W., Wu, X.R., 2012. Weight functions and strip-yield model analysis for three collinear cracks. *Eng. Fract. Mech.* 85 (1), 73–87.